V. Epshteyn , P. Shatalov (ITEP) ATLAS-FCAL beam tests 2003 Note4, 2003-10-30
Last update: 19/11/2004, with P. Gorbunov (U. of Toronto & ITEP)

The analysis status report

1. Introductory remarks

- **Event selection:** the same for electrons and pions
  - ✓ PH(muon counter)<15,
  - ✓ PH(veto counter)<15,
  - ✓ $0.5 < counters\_signal < 2$, $\qquad counters\_signal = \frac{1}{3}\sum_{i=1}^{3}\frac{PH(counter)_i}{median(PH_i)}$
  - ✓ left (right) in BPC(1,2,5,6)<1990,
  - ✓ The corresponding co-ordinates (X, Y) in adjacent beam chambers (1 and 2, 5 and 6) should not differ by more than 1 mm.
  - ✓ Area cut in all beam chambers: |X, Y|<40 mm.

  Remark: the Gaussian parameters μ and σ for the energy distributions peaks are practically insensitive to the event selection cuts.

  For muons: the same, except PH(muon counter)>20.

- **Calorimeter response R**.
  For electrons, only FCAL1 is used (FEBs 7 and 6). A longitudinal leakage is absent. Even at 200 GeV/c adding FCAL2 does not change the average. For pions, all modules are used:

$$FCAL1(FEB\#7,6) + g2 \cdot FCAL2(FEB\#5) + g3 \cdot FCAL3(FEB\#1,0), \quad g2, g3 = 2.$$

  The weights g2, g3 are tuned to optimize the pion resolution (see [1]).

  Two options are used to compute the total calorimeter response:
  R_total – a sum of amplitudes over all FEB channels
  R_core – a sum of amplitudes in the tiles whose centers (taken from Mike's table) are strictly inside a cluster with the radius *r_core*, with the cluster center determined by the beam chambers[1].

  The mean response μ and the resolution σ quoted in this Note are determined by a Gaussian fit to the peak of the measured energy distribution for the corresponding beam condition.

- **Signal amplitude**. We have samples $\mathbf{S_{0\text{-}6}}$ and the corresponding ADC readings $\mathbf{A_{0\text{-}6}}$. In the previous notes we considered three methods to determine the signal amplitude:
  - ✓ *parabola* – from a parabolic fit of $\mathbf{A_{2\text{-}4}}$;
  - ✓ *raw* – max($\mathbf{A_{2+4}}$);
  - ✓ *spline* – the $\mathbf{A_{2\text{-}5}}$ values are fit with a cubic spline (this method was shown to give the smallest quantization noise).

  In this Note two more methods are considered:
  - ✓ *spice* – a fit of $\mathbf{A_{2\text{-}5}}$ values with the shape obtained by a PSpice simulation of the read-out channel response to a triangular tube signal (*including a detailed tube and amplifier models*);
  - ✓ *raw_1* – $\mathbf{A_3}$ is taken as the amplitude.

[1] In the previous notes the cluster center was defined as the center of the tile having the highest signal. This method was good for electrons with energies down to 10 GeV and for pion energies greater than 60 GeV. An application of this method at lower energies (e.g. at 5 GeV) is limited by the noise.

In the table below, these methods are compared for electrons at 100 GeV/c, for position 4L, and *r_core*=8 cm (runs 3429-3432). The total noise per sample within the cluster – 17 ADC counts:

procedure	raw_1	spline	spice
μ, ADC counts	1099	1129	1148
σ, %	7.53	5.09	4.69

Statistical errors are negligibly small.

The spline and spice methods are clearly better than raw_1. The spice method features the minimal quantization noise contributing to the constant term of the energy resolution. But in this example the electronic channel is relatively small: ~1.7% (17/1000). What can we expect if the relative noise gets larger (e.g. at lower energies)? The signal shape averaged over a large number of events remains unchaned. But on event-by-event basis the noise can distort the shape and lead to a systematical bias of the reconstructed amplitude.

To study this issue, one cannot just measure μ and σ at a lowest energy, since *a priory* the correct result is unknown. Therefore, we increased the relative electronic noise artificially, event-by-event, by adding a simulated electronic noise to the recorded data[2].

Naturally, the resolution deteriorates with the higher noise. The bad thing is that the reconstructed mean response is changing, too, as Fig. 1 shows. For a linear system, μ should be insensitive to the noise and this is almost the case for the *raw_1* method. On the contrary, the *spline* method exhibits a strong dependence on the relative noise, which will result in a potentially large systematical error at low energies. Actually, to some extent, all the considered methods suffer from this problem. However, the fit conditions in the *spice* method can be adjusted in such a way as to minimize the bias[3]. Alternatively, one can resort to the *raw_1* method, but the energy resolution will suffer.

Bottom line*: the spice method is used for the results presented in this Note*, except for muons (Section 4)

- **Expected noise**. The effective reconstructed noise can differ from the measured pedestal noise (an rms scatter of the ADC value in absence of an input signal). To study this issue, we added a constant signal shape obtained with PSpice to real pedestal events and found the effective noise value from the distribution of reconstructed amplitudes. The expected noise values quoted further in the text are obtained with this method.

- **The electronic calibration is not used, so far.**

2. Electrons

All the tables are available but I do not include them in order not to encumber the text. A circular cluster area of the radius *r_core* = 8 cm contains ~99% of the deposited energy. The corresponding **R_core** distributions for position 4L are shown in Fig. 2.

Commentaries:

- **Energy dependence of the response** (position 4L) is quite linear (Fig. 3).
  With all runs used: $R = 11.71 \cdot P - 12.68$, *[P]=GeV/c. [R]=ADC counts*
  With September runs only: $R = 11.56 \cdot P - 6.933$.

[2] The noise simulation is done with PSpice, with the noise spectral characteristics typical of the FCal read-out channel. A detailed description of the noise model and how the simulated noise was translated into the ADC samples is beyond the scope of this report and can be a subject of a separate note. The relative noise contribution was varied by changing the average magnitude of the primary noise.

[3] This brings us to the OF method, which is nothing else but a linearized form of the *spice* method .

The reason for splitting the data into two groups (all runs and September runs) is that the electron beam appears to be fairly different in these two periods. This is seen in Fig. 2: the spectra for P=150, 200GeV/c have a significant right tail. Further difference between these two groups will be shown below.

There is an offset of ~1 GeV, which can be attributed to a non-linear energy dependence of a sampling calorimeter response at lowest energies, when electromagnetic showers are not fully developed yet. To validate this statement MC simulations are needed.

- **The calorimeter resolution (**position 4L), Fig. 4. Because of the difference in September and July data, I quote only the results for September runs. The fitted resolution curve is a quadratic convolution of three terms:

$$\sigma = a \oplus \frac{b}{\sqrt{P}} \oplus \frac{c}{P},$$

a=(3.74±0.19)%, b=(25.2±1.97)%, c=(143±3.6)%, [P]=GeV/c.
The fitted noise term c is in a good agreement with the measured (expected) noise of 16.7 ADC counts corresponding to (16.7/11.6)≈1.44GeV/c.

The values of the constant and stochastic terms are quite acceptable. However, the question remains: why September and July runs are so different? Fig. 5 reveals a weird structure along the X- axis for –150 and –200 GeV runs, which is absent in September runs. It is this structure that leads to a worse resolution. Where it comes from is unclear: further work is needed.

- **The distribution shape ─ the tails.**

Left tail. A certain fraction of it is due to pions: see Fig. 6. Adding FCAL2 κ FCAL1 does not change the signal magnitude, i.e. the whole electron energy is deposited in FCAL1. However, an upper cut on the FCAL2 signal helps to reduce the number of events in the right tail. The Gaussian-fit parameters for FCAL1 do not depend on this cut. The origin of the remaining events in the left tail is unclear – they can be either due a beam anomaly, or due to remaining pions fully contained in FCAL1. Or, possibly, this is just the way FCAL1 works. A study will be continued.

Right tail. A deviation of the right part of the peak from a Gaussian develops with the increasing energy (Fig. 2). This deviation washes out if *r_core* is increased (Fig.7). If all FCAL1 channels are included, an almost Gaussian shape is restored, presumably, due to an increased contribution of the random noise. To check this, the total FCAL1 noise was added to the signal shape for *r_core*=8cm. The resulting distribution (Fig. 7D) is very similar to the **R_total** distribution, Fig.7C. A study to identify the nature of the right tail is in progress.

- **Variation of the calorimeter response across FCAL1.**

Figure 8. The tiles of 4×4 tubes in the beam region (position 4L), with the total number of hits >1000, have been selected. The scatter of the response to electrons hitting different tiles[4] is 3%. This can be either due to the geometry, or due to the electronic gain variation. As was mentioned in Section 1, the electronic calibration is not applied to the results presented in here. It is desirable to clarify the origin of this scatter. If it is not due to the gain variations, this can limit the accuracy of the calorimeter calibration.

Figure 9. The X-Y structure of the FCAL1 response **R_core(8cm)** is shown for the tile most illuminated by the beam. Though the picture is smeared (because the beam is not parallel to the tubes), the structure of a regular FCAL1 tile is quite visible. The calorimeter response depends on whether argon or the absorber is hit by the beam electron.

[4] The tiles are not exactly rectangular, but this does not affect the conclusions.

Figure 10. The tile geometry is such that individual tubes are staggered in X-direction and fully overlap in Y-direction. Respectively, one observes different dependences of the calorimeter response on X- and Y-positions of the impact point within one tile. In the X-dependence, the contributions of overlapping copper and argon regions are averaged out, while in the Y-dependence the tube structure (illustrated by Fig. 11) is clearly seen. There are Y-positions with copper only (B) where the response drops, and the ones "enriched" with argon (A, C) where the response is higher. In position D the copper dominates and the response is similar to the one of position B.
This structure defines the irreducible constant term of the energy resolution, provided the electronic gain variations can be corrected.

- **Position 4H.** Beam positions 4L and 4H differ by a presence an extra absorber in the 4H series.

Energy dependence of the response. Fig. 12 shows the energy dependence of the response:

$$R = 11.77 \cdot P - 20.52, \quad [R] = ADCcounts, [P] = GeV/c$$

Within a percent, the linear factor equals the one for 4L, but the offset, expectedly, is larger: ~2 GeV (20.52/11.77).

Energy resolution – Fig. 13:

$$\sigma = a \oplus \frac{b}{\sqrt{P}} \oplus \frac{c}{P},$$

a=(3.7±0.4)%, b=(22.1±5.7)%, c=(176±7.7)%, [P]=GeV/c.

Both constant and stochastic terms are the same as for 4L, while the noise is higher (~1.8 GeV), due to the presence in these runs of the extra noise from the pulser ("modulo-8" effect).

3. Pions

Tables are not incuded. *r_core*=16cm contain >97% of the deposited energy. The **R_core(16cm)** distributions are shown in Fig.14.

Commentaries:

- **Energy dependence of the response,** Fig. 15.

$$R\_core(16cm) = 9.818 \cdot P - 29.57, \quad [P] = GeV/c, [R] = ADC\ counts$$

For some reason (to be investigated!) the point 20GeV/c is distinguished. The impression is that the beam momentum here is not 20 GeV/c but rather 25 GeV/c (this is also suggested by Fig. 16).
The offset is bigger than for electrons: 29.57/9.818 ≈ 3 GeV. This can be expected, because hadronic showers start fully developing only at the energies of a few GeV.

- **The energy resolution**, Fig. 16. The fit by a usual form

$$\sigma = a \oplus \frac{b}{\sqrt{P}} \oplus \frac{c}{P}$$

is of is significantly worse quality than for electrons. The fitted parameters are: *a=(3.1±3)%, b=(112±43)%, c=(783±228)% ([P]=GeV/)*

In principle, one can expect a smaller constant term than for electrons, because of a larger shower volume. The signal is always averaged over a large number of tubes and the X-Y structure typical of electrons is absent. However, it is currently impossible to evaluate *a* for pions more accurately.
.
The fitted noise term *c* is compatible with the direct noise measurement of 70 ADC channels: 70/9.8 ≈7GeV (700%).

The 100 GeV/c point is plagued by the modulo-8 effect. The 20 GeV/c point is anomalous, as was mentioned earlier.

- **Energy distribution shape, the tails**, Fig. 14

  The left tail is interesting: is it a beam anomaly or a feature of the calorimeter? It is unclear, needs to be investigated.

  Right tail. Like for electrons, the deviation from a Gaussian shape grows with the beam energy. Similarly, we observe a better Gaussian shape for larger *r_core* , Fig. 17.

4. Muons

Fig. 18 shows the distributions for muons in FCAL1 (P=-200GeV/c, runs# 2890-2896). The raw_1 method is used for the signal amplitude. There is nothing interesting here. The signal is small: ~0.9 GeV; the left part of the peak is purely Gaussian (=pure noise).

5. Conclusions

1. The "*spice"* method of signal amplitude determination gives the best resolution and is almost unbiased.
2. MC simulations are needed to interpret the observed features, like the response offset and non-Gaussian tails of the response distributions.
3. The electronic channel noise amounts to
   - ~1.5 GeV for electrons (FCAL1 only, *r_core*=8 cm)
   - ~7-8 GeV, for pions (the entire calorimeter, *r_core*=16 cm)
4. The "150 and 200 GeV" anomaly in electron runs needs to be investigated. A hint: the structure in X-dependence of the FCAL1 response.
5. The tile-to-tile variations of the FCAL1 response have to be understood. Gain variations?
6. The "20 GeV" anomaly for pions. Can it be to a wrong beam energy attribution?
7. A fine structure in the electron response, related to the tube structure of FCAL1, is observed. It imposes a lower limit on the constant term of the electron resolution.

Figures

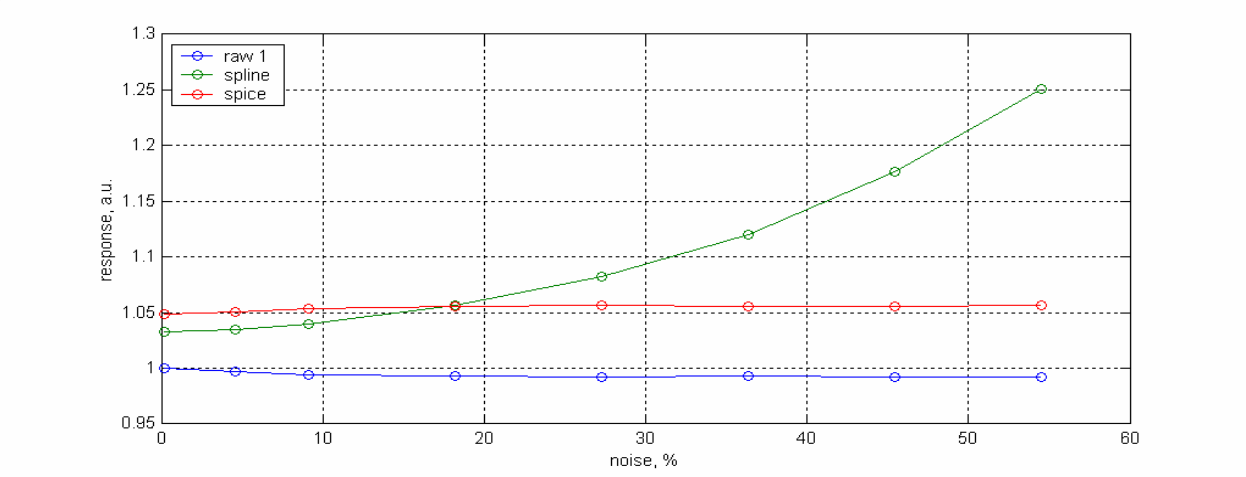

Figure 1: The influence of noise on the the calorimeter response, for different methods. All points are normalized to the case of *raw_1* response with no extra noise

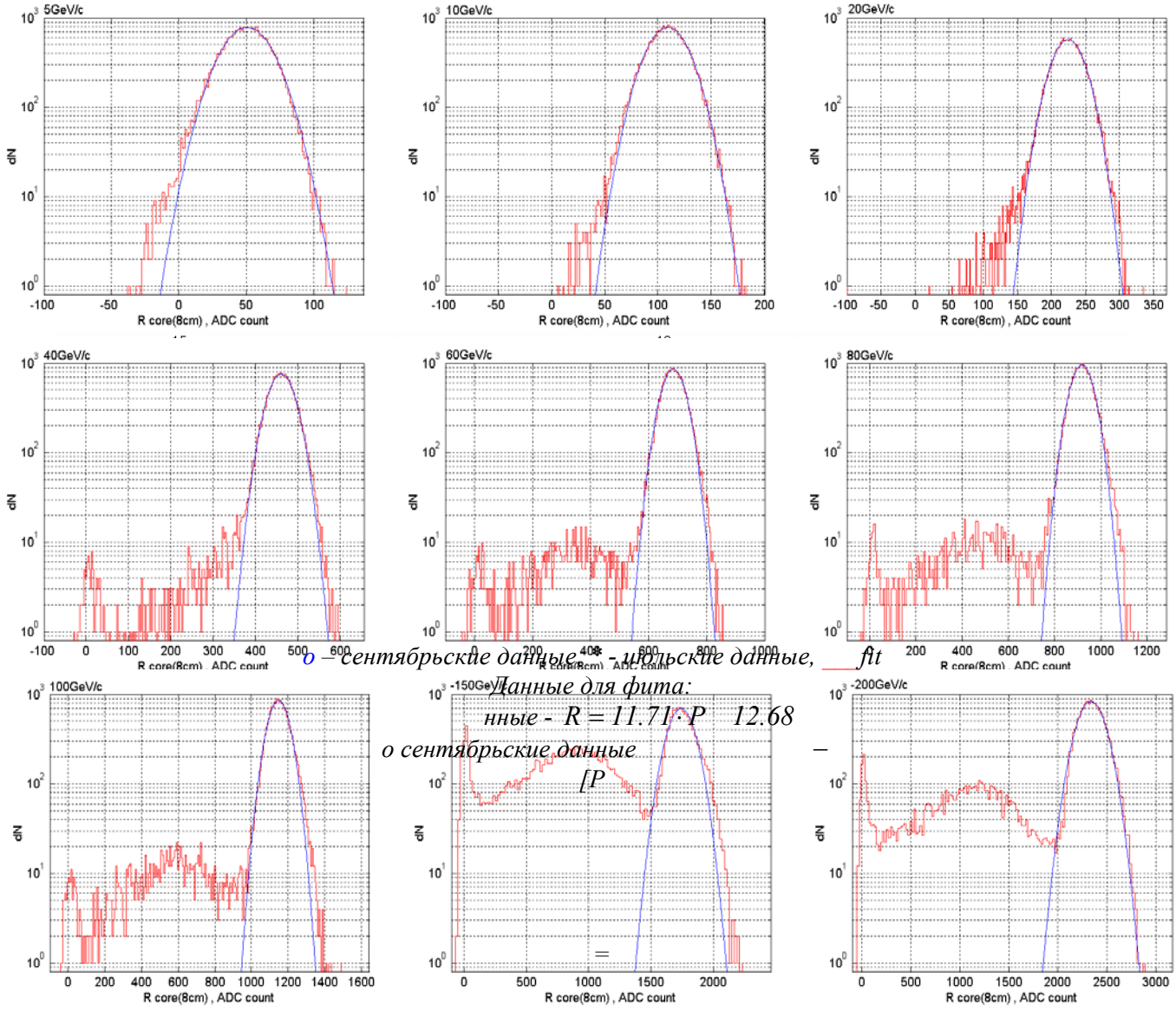

*o – сентябрьские данные, * - июльские данные, ___ fit*

Данные для фита:

нные - $R = 11.71 \cdot P \quad 12.68$

о сентябрьские данные

[P

Figure 2: R_core(8cm), for electrons (4L). ___ data, ___Gaussian fit.

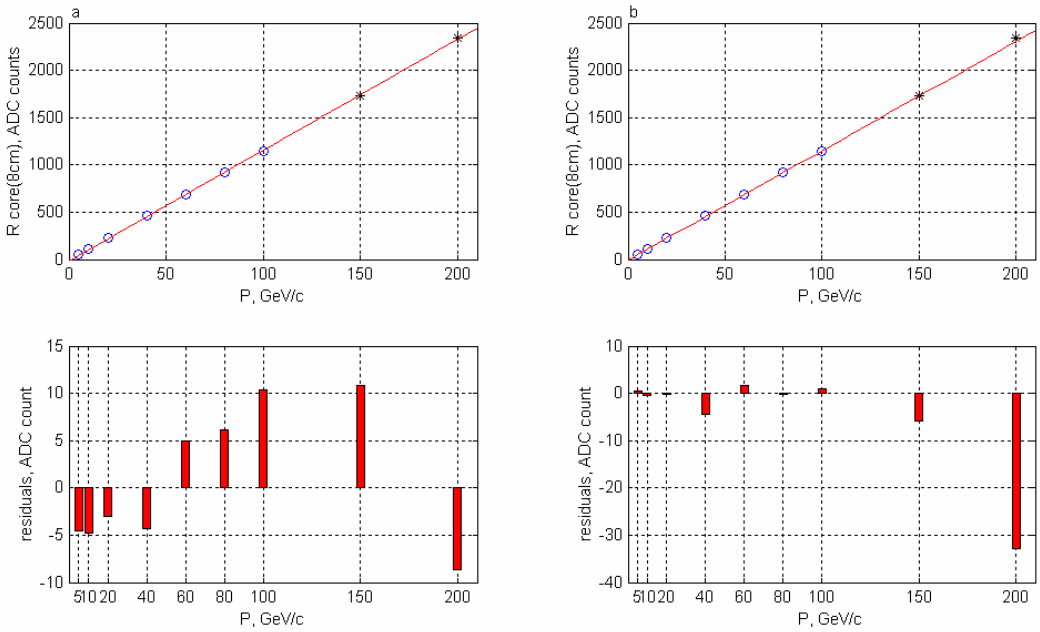

Figure 3: FCAL1 response to electrons, **R_core(8cm),** position 4L.
○ – September runs, * - July runs, ___ fits

a – fit using all data, b – fit using September data

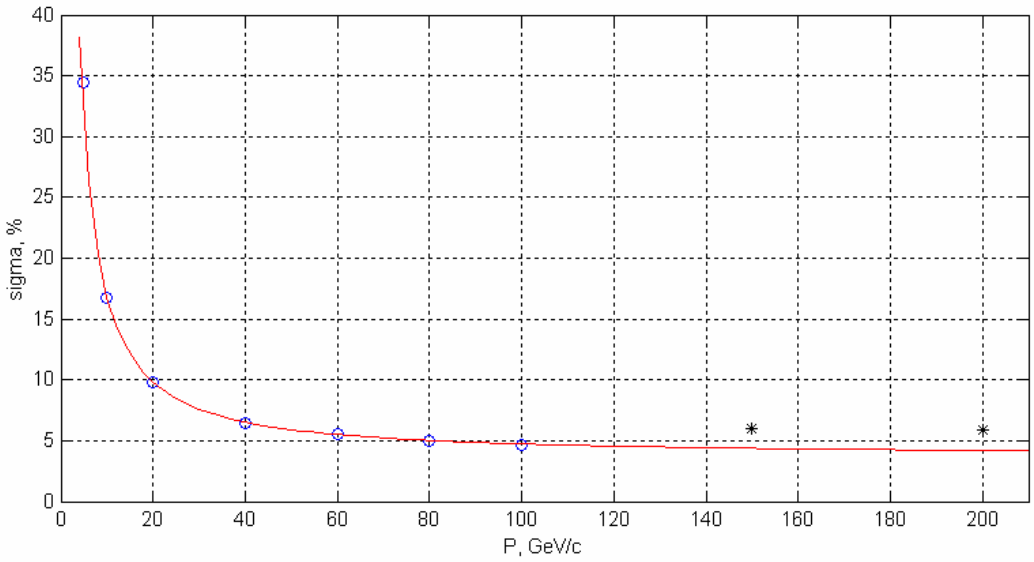

Figure 4: FCAL1 energy resolution (**R_core(8cm),** electrons, position 4L)
○ – September runs, * - July runs, ___ the fit to September runs only (see text)

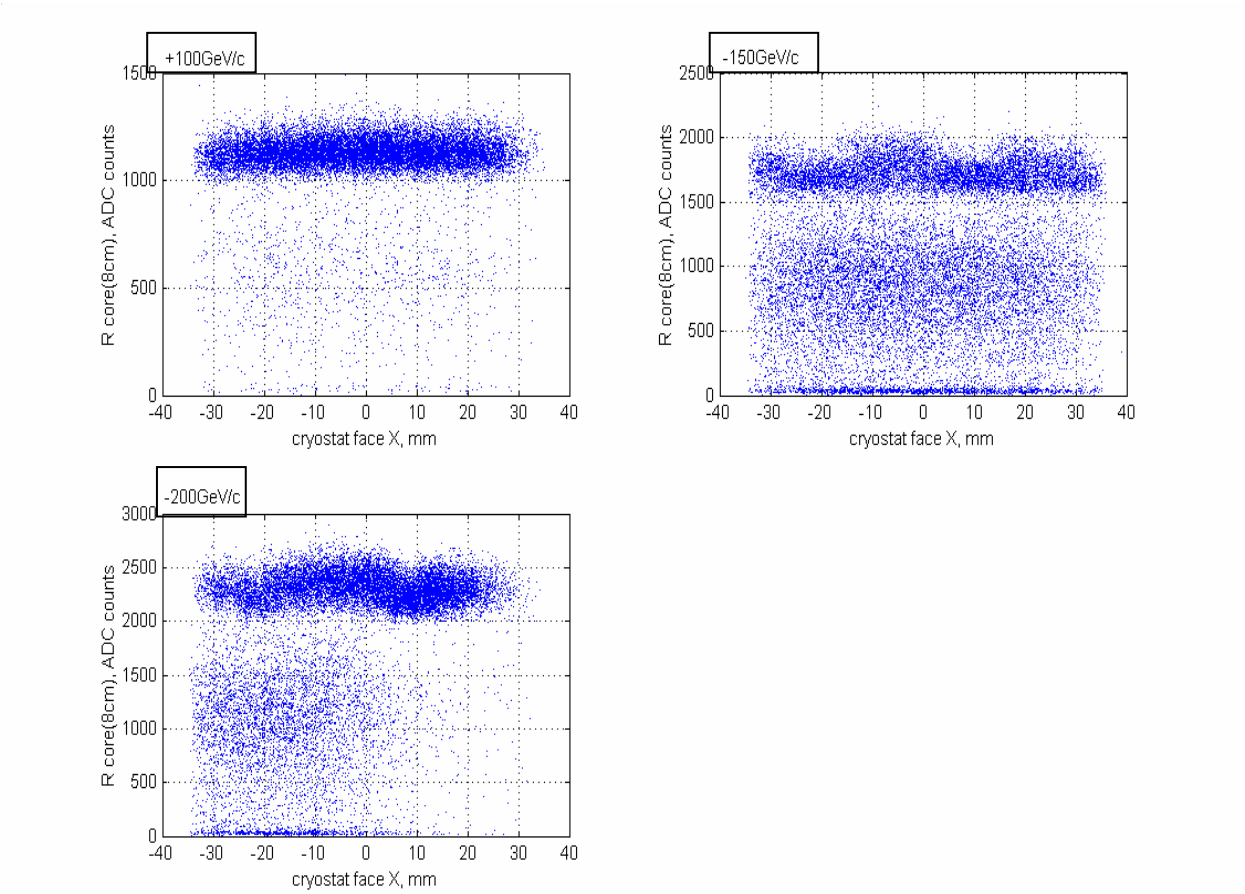

Figure 5: R_core(8cm) vs X coordinate on the cryostat front face, for different beam energies. Electrons, position 4L, P=+100, –150, –200 GeV/c.

Puc.5

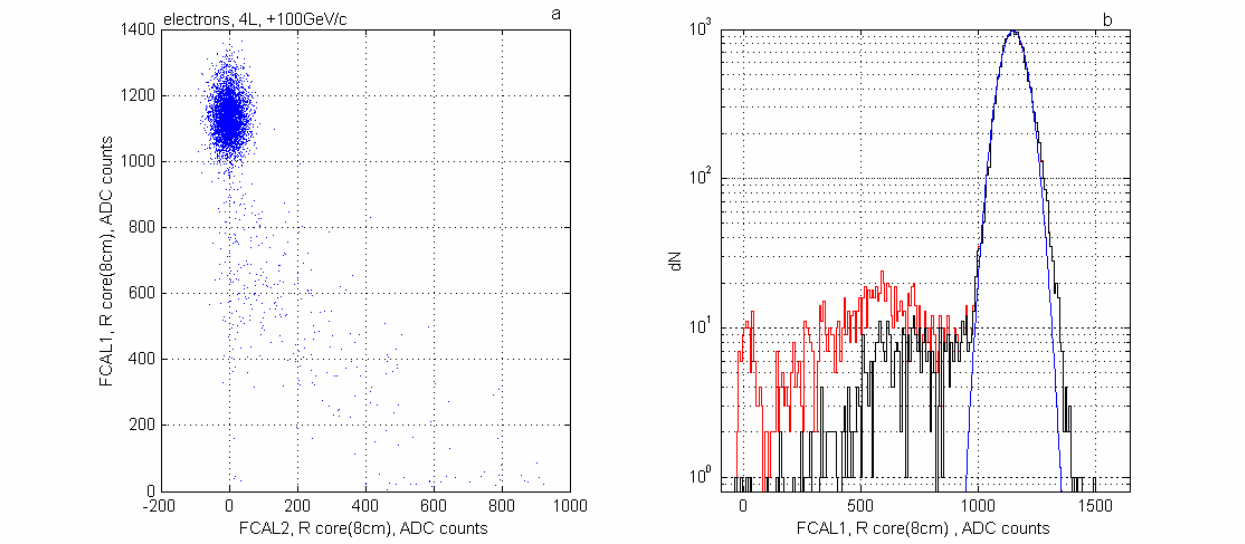

Figure 6: (a) FCAL1 vs FCAL2;
(b) the effect of the cut **R_core(8cm)** <80 ADC counts in FCAL2 on the left tail of the FCAL1 response; ___without cut, ___ with cut.

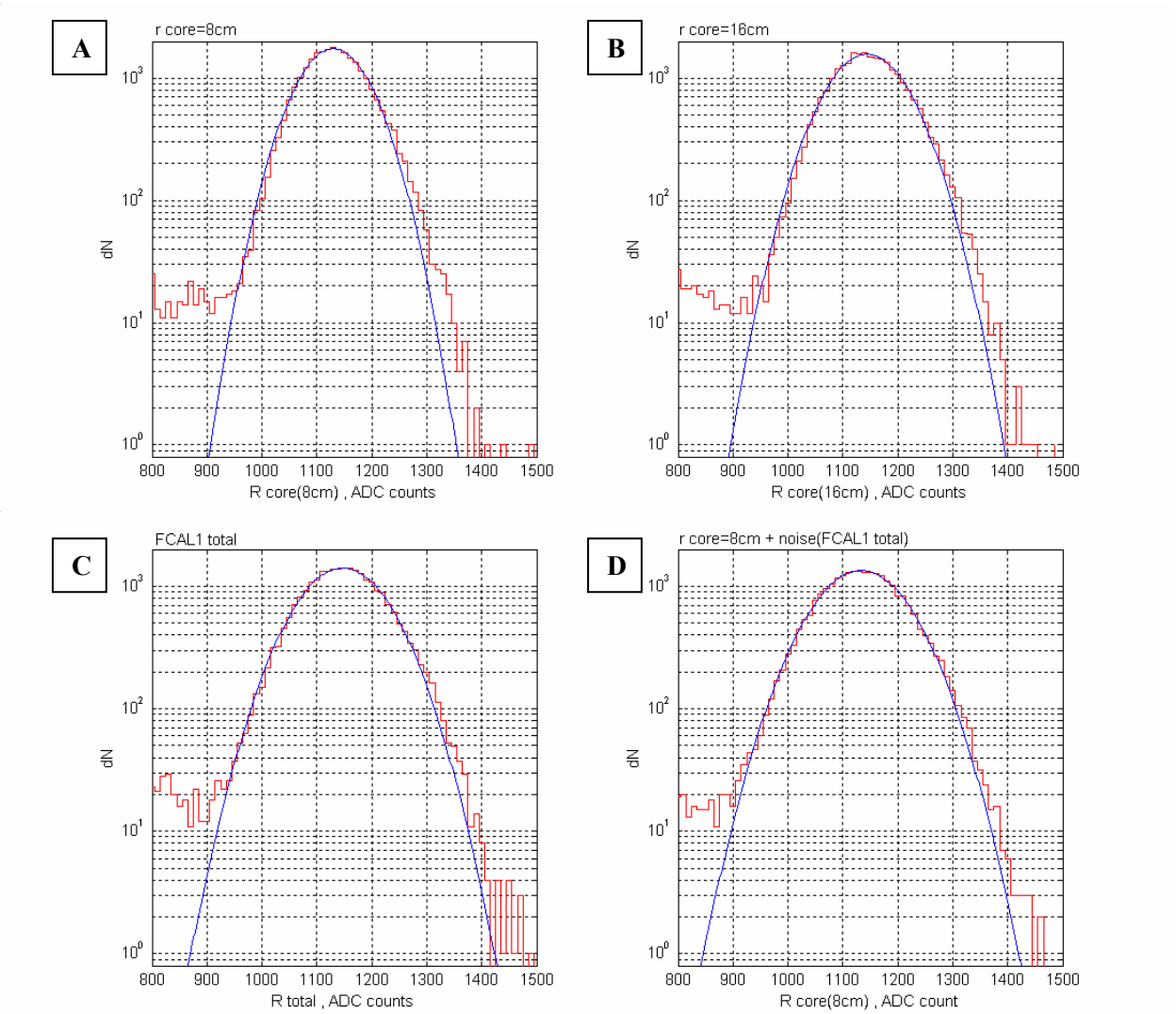

Figure 7: R-distributions, electrons, position 4L, 100GeV/c, for different *r_core*.
___ data, ___Gaussian fit.
(A) 8cm; (B) 16cm; (C) the entire FCAL1; (D) 8cm + additional noise

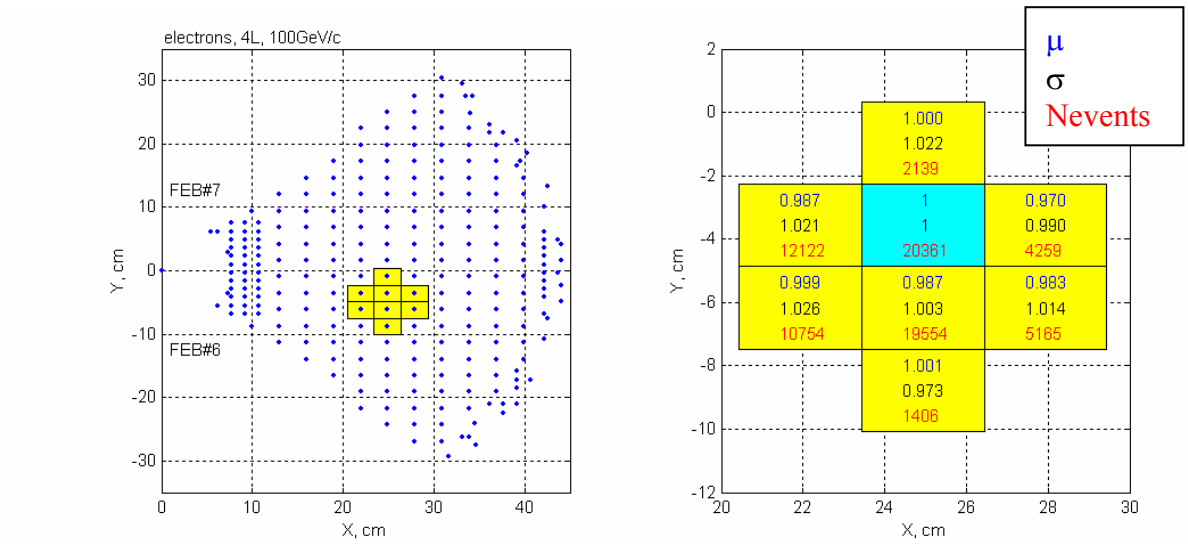

Figure 8: R_core(8 cm) for different tiles around the beam axis
X, Y – coordinates of the beam impact point.

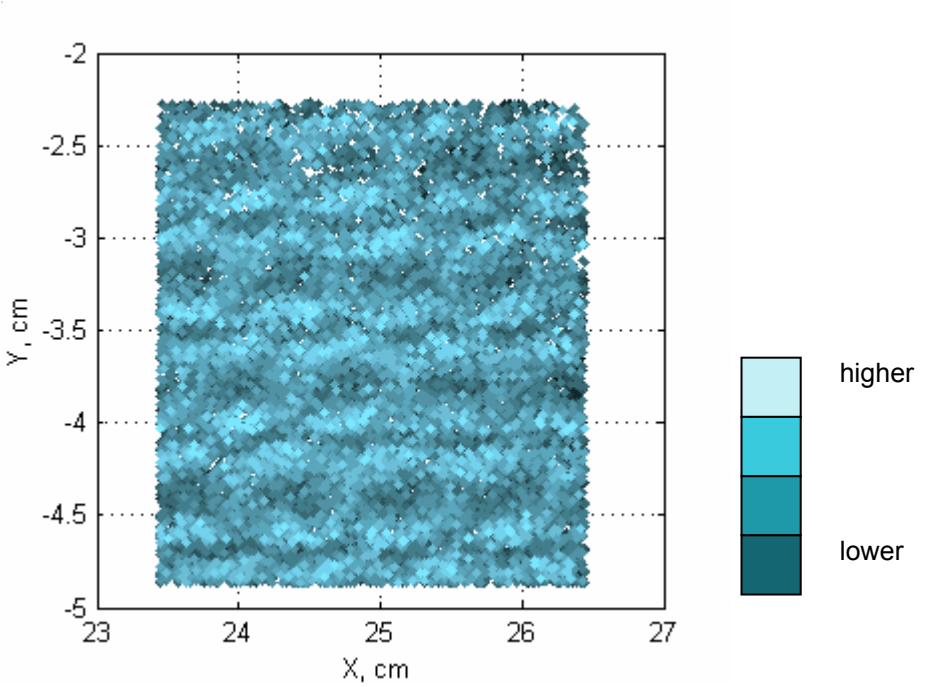

Figure 9: A variation of the FCAL1 response **R_core(8cm)** over one tile surface.

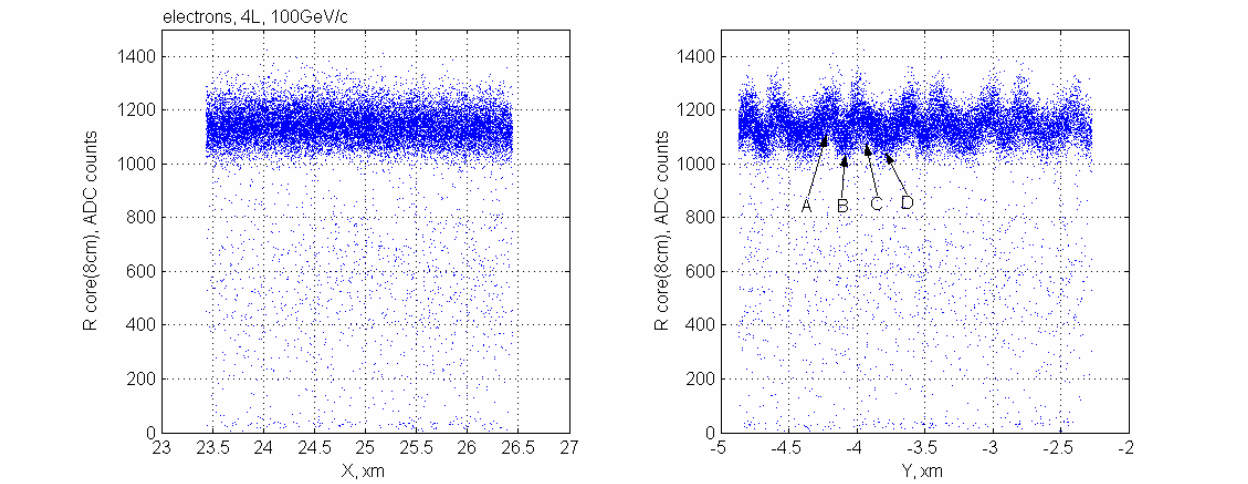

Puc.10. FCAL1 response vs. X- and Y- coordinates over one FCAL1 tile

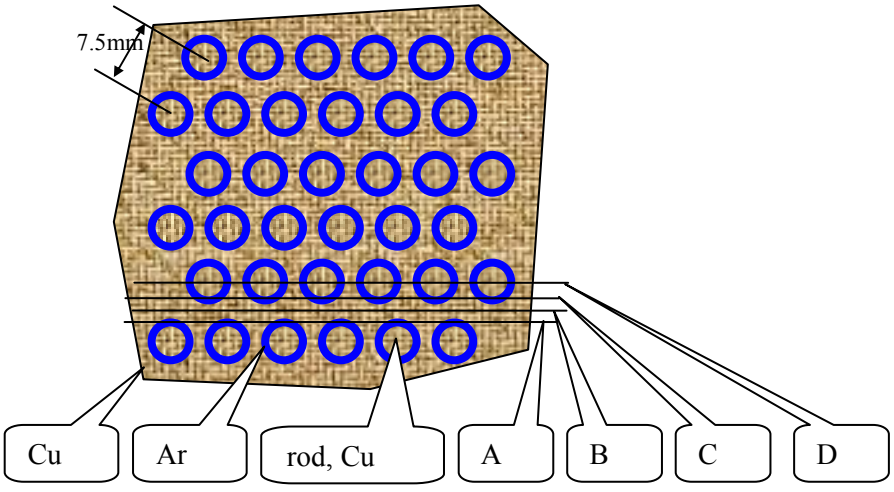

Puc.11. FCAL1 tube structure

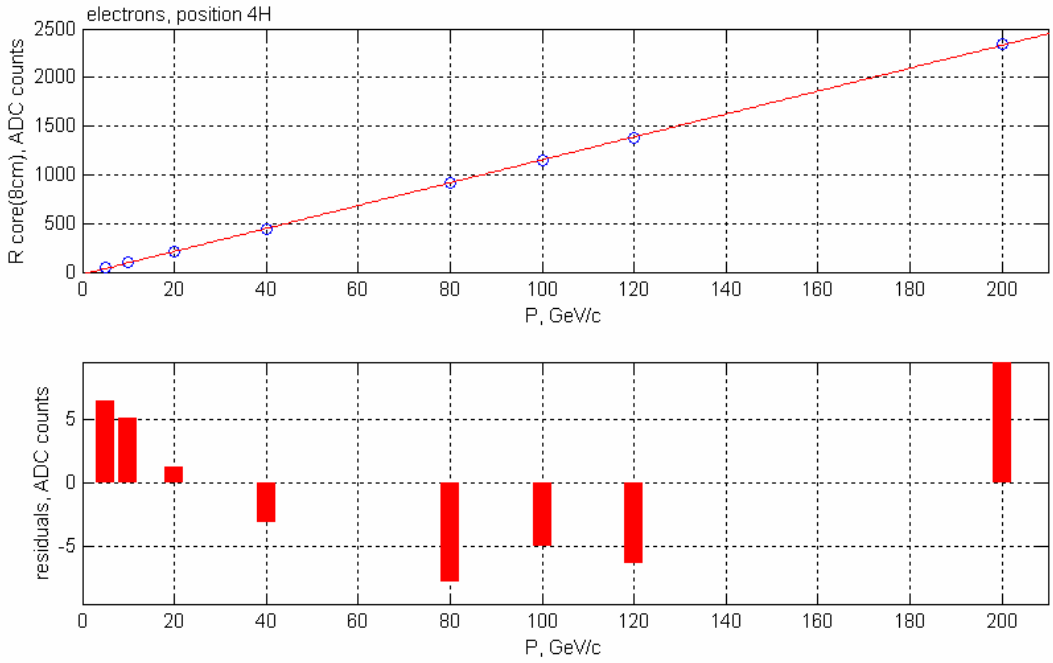

Figure 12*:* FCAL1 response to electrons**, R_core(8cm**), electrons, position 4H
○– data, ___ fit

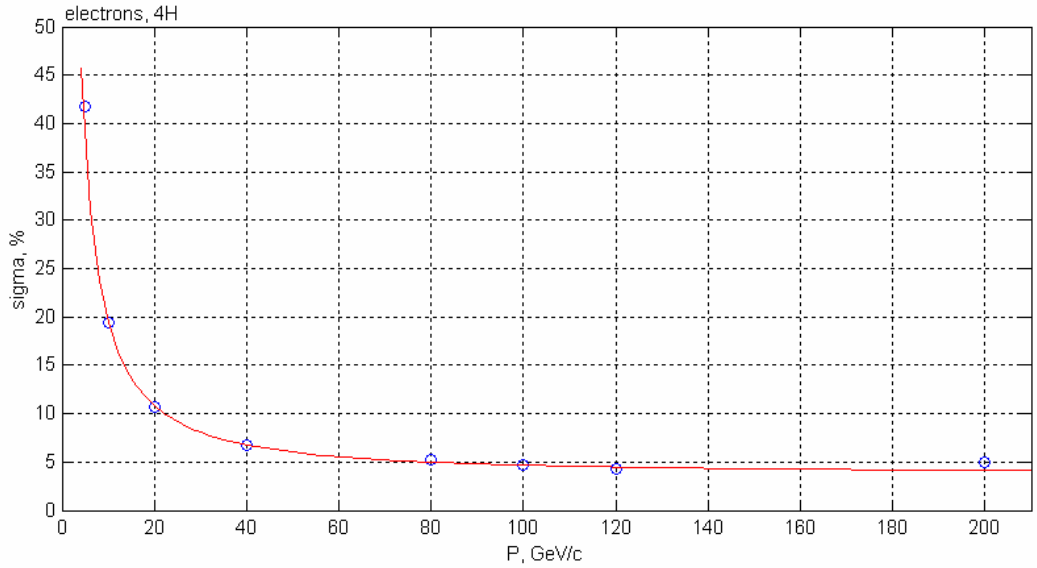

Puc.13. Energy resolution, **R_core(8cm)**, electrons, position 4H.

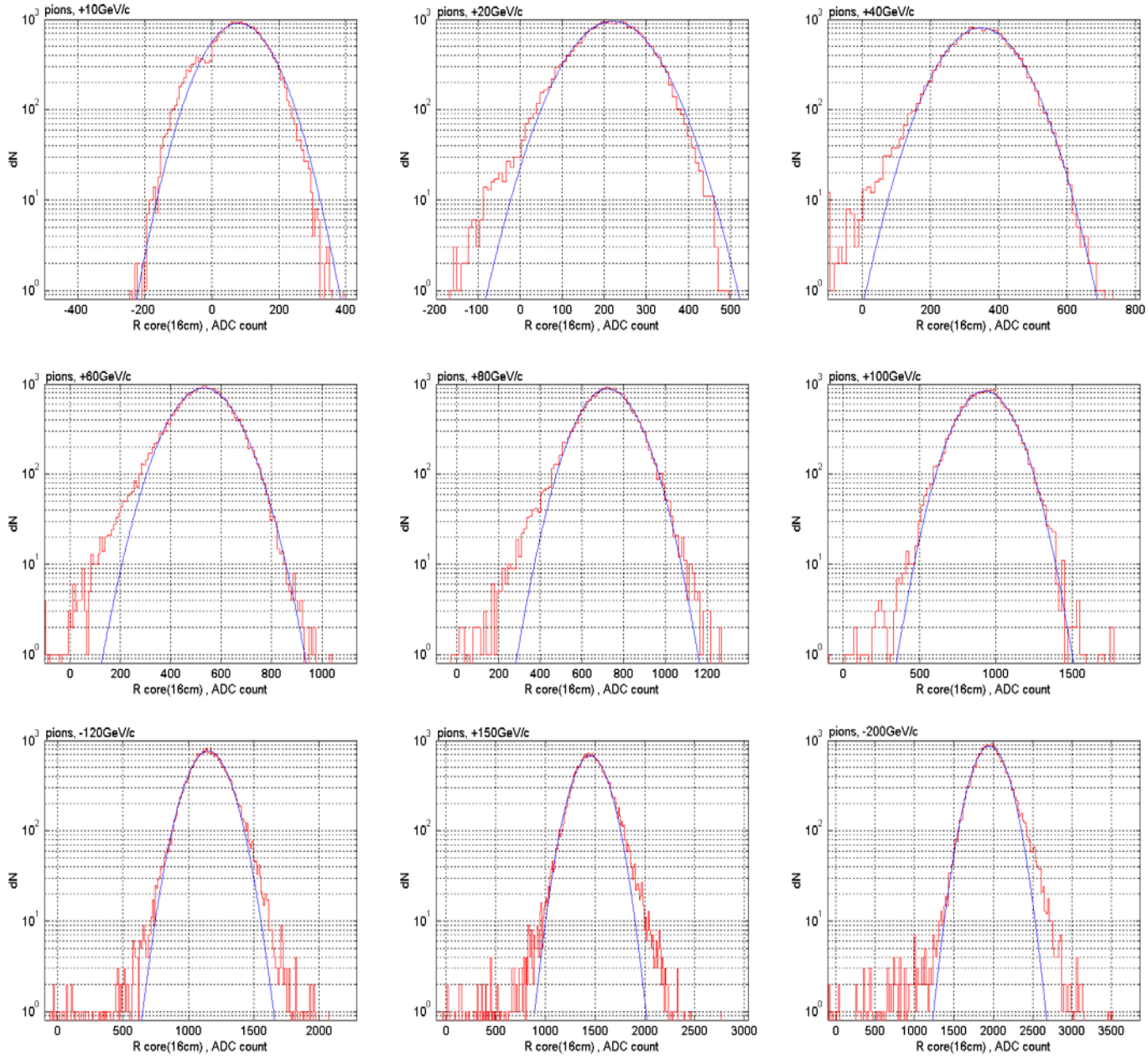

Figure 14: R_core(16cm) distributions for pions, position 4L.

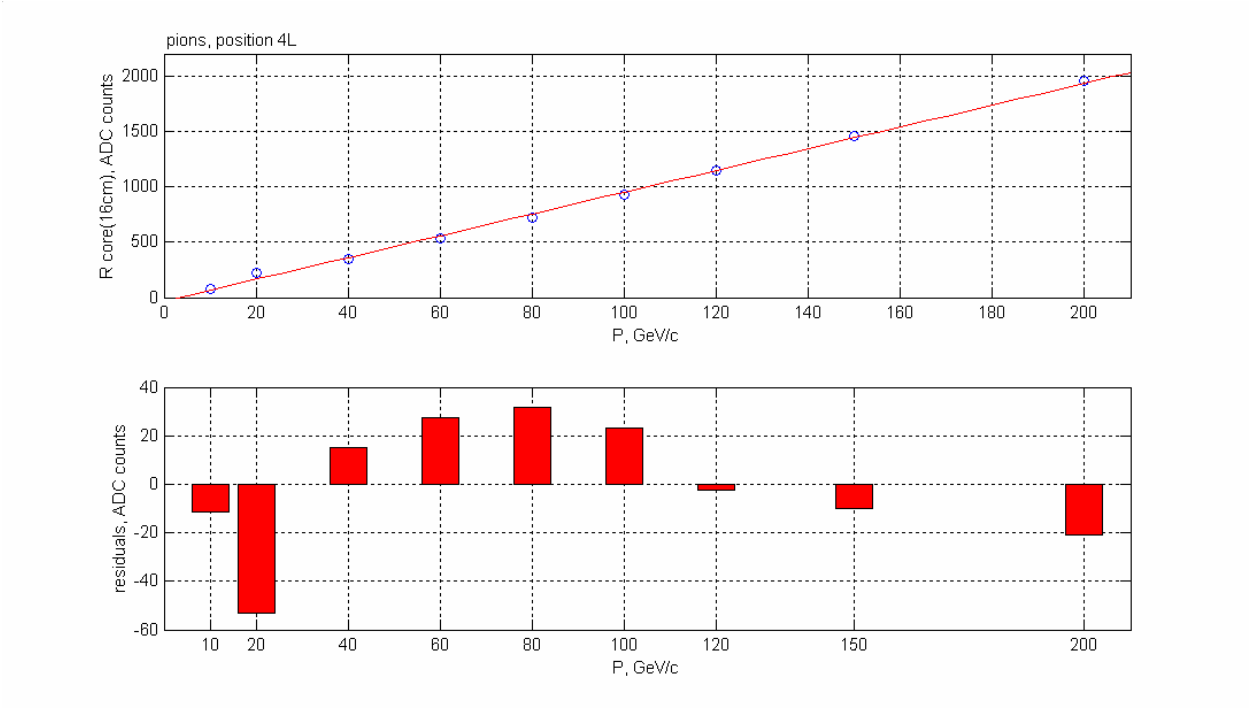

Figure 17: The response for pions, position 4L .

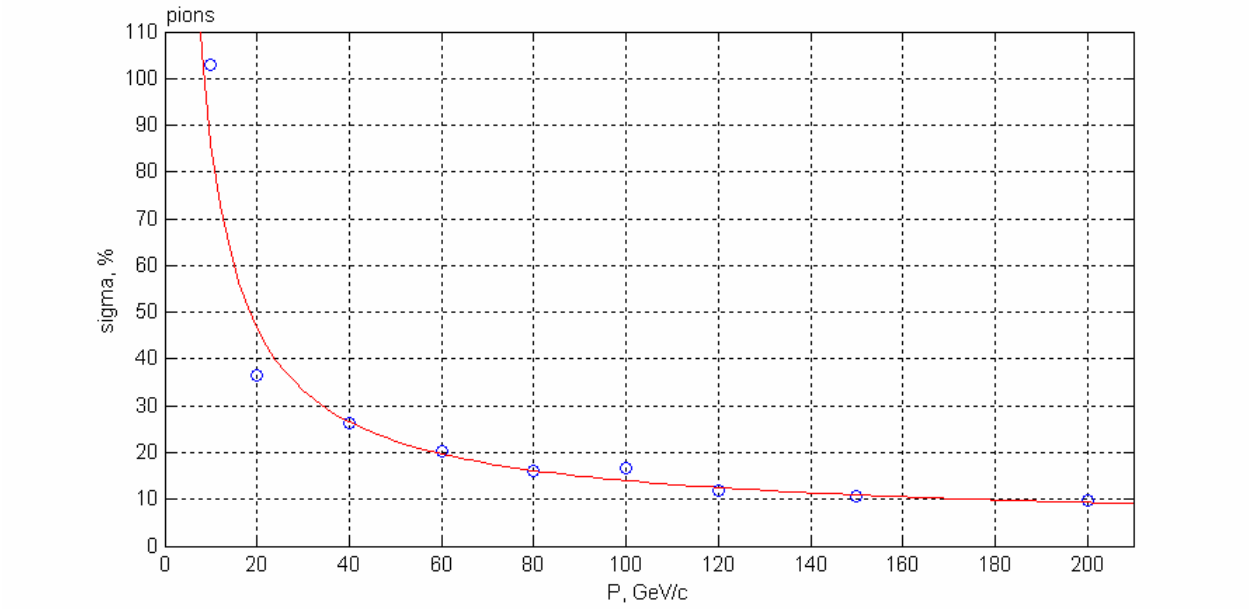

Figure 16: Energy resolution for pions, position 4L.

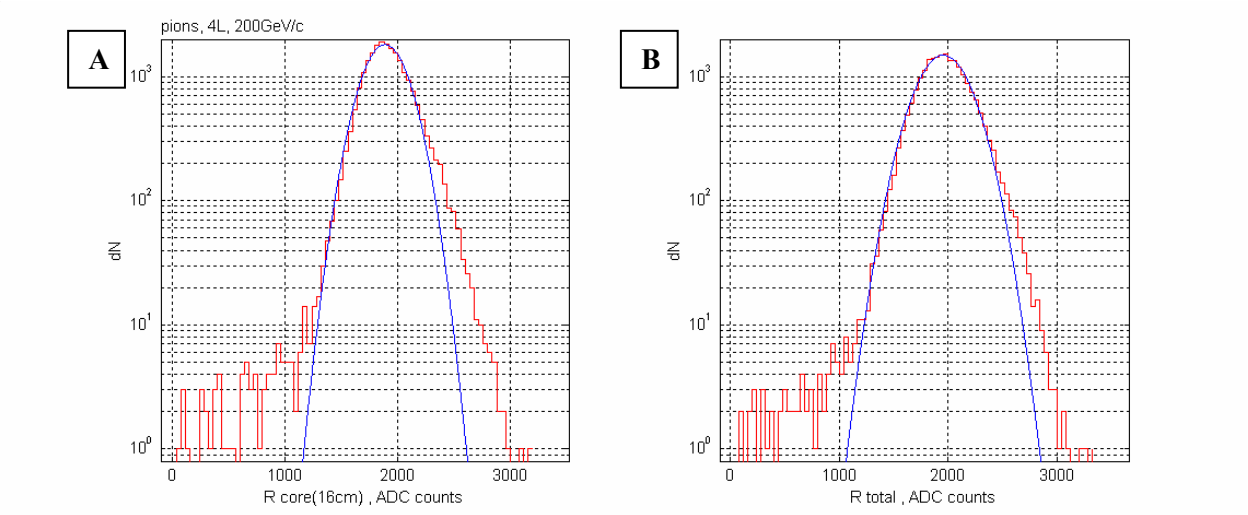

Figure 17: R-distributions, pions, position 4L, 200GeV/c
___ data, ___Gaussian fit.
r_core: A – 16 cm, B – the entire FCal

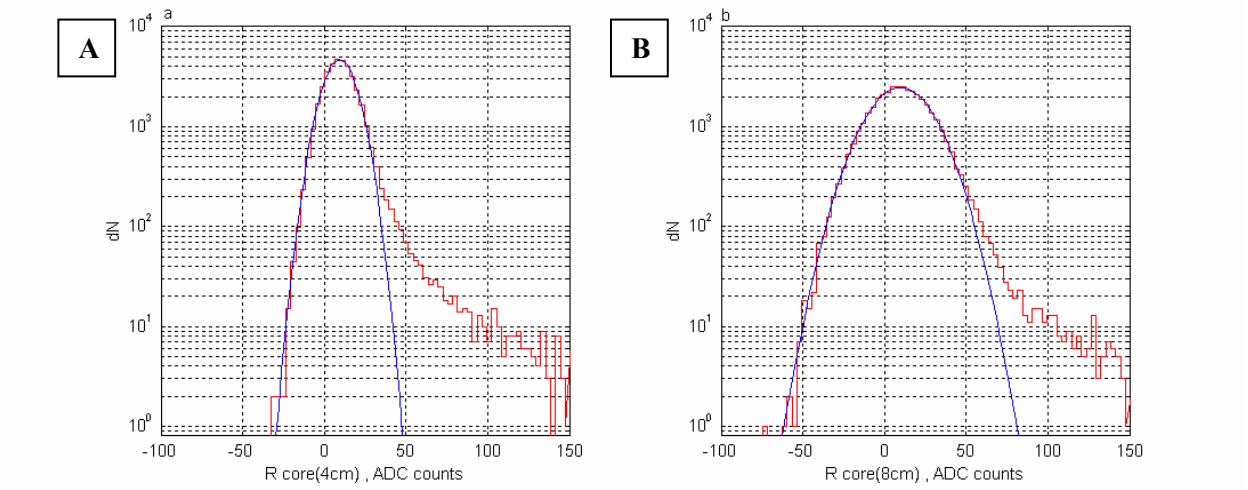

Figure 18: Total response for muons, 200GeV/c
r_core: A – 4cm, B – 8cm.